PROCEEDINGS, 48th Workshop on Geothermal Reservoir Engineering
Stanford University, Stanford, California, February 6-8, 2023
SGP-TR-224

WHOLESCALE - Calibration and Simulation of hydro-mechanical Behavior at San Emidio, Nevada During Operational Changes

Michael A. Cardiff, Chris Sherman, Hao Guo, Erin Cunningham, Matt Folsom, John Murphy, Ian Warren, Hiroki Sone, Cliff Thurber, Herbert F. Wang, and Kurt L. Feigl

Mailing address: UW-Madison Department of Geoscience, 1215 W. Dayton St., Madison, WI 53706 USA

E-mail: cardiff@wisc.edu

Keywords: WHOLESCALE, San Emidio, Inverse Modeling, Pore Pressure

ABSTRACT

Changes to geothermal pumping operations produce changes in reservoir fluid pressure that propagate according to the arrangement of fluid sources / sinks (injection / extraction wells, respectively) and reservoir permeability. These changes in fluid pressure induce changes to effective stresses acting on potential fault planes, and thus alter fault stability. For example, Cardiff et al. (2017) used a semi-analytical model, calibrated on existing pressure data, to simulate pressure changes during temporary cessations of pumping when a geothermal plant was shut down for maintenance. They demonstrated that microseismic events observed post-shutdown occurred where predicted fluid pressure increases (and effective stress decreases) between 0.05 MPa - 0.15 MPa were simulated. This work investigates pressure changes associated with similar site shutdowns at the San Emidio Geothermal Field, Nevada. Using existing pumping and pressure change data, we have calibrated finite element numerical models based in the COMSOL and GEOSX platforms. Following calibration, we simulate expected pressure changes and stress field changes within the San Emidio reservoir during site shutdowns. A catalog of microseismic event times and locations measured before, during, and after shutdown can be compared against the spatiotemporal changes in fluid pressures and effective stress simulated by our models. In theory, once properly calibrated these models allow the prediction of future seismicity as site operational changes are implemented, such as new pumping wells or flow rate adjustments. In this paper, we provide a snapshot of work in progress. The work presented herein has been funded in part by the Office of Energy Efficiency and Renewable Energy (EERE), U.S. Department of Energy, under Award Number DE-EE0009032.

1. INTRODUCTION

Most currently-viable geothermal reservoirs exist in areas of significant faulting or fracturing, where permeability introduced by these features allows deep geothermal heat to be advected to shallower depths. Faulting and fracturing over-prints new structures of permeability on top of existing permeability present in the host geologic material (i.e., host rock). Whether dominated by fault / fracture systems or by other pre-existing permeability in host rocks, the structure of fluid permeability represents a key control on fluid flow pathways, heat transmission, and effective stress changes caused by pumping. Determining permeability distributions in the subsurface is thus a key prerequisite to accurate simulation of reservoir stress changes.

The San Emidio geothermal reservoir, near Fernley, Nevada, USA (Figure 1) is located within a “classic” Basin and Range structural system dominated by normal faulting and interaction with dextral strike-slip motion of the nearby Walker Lane fault system (Faulds et al. 2005; Folsom et al. 2020). Locally, right-stepping bends in faults are thought to produce dilation and permeability that allows pathways for geothermal heat and fluids. Broadly, these structural settings of fault “step-overs” or “relay ramps” have been identified as creating favorable conditions for geothermal power generation throughout the Great Basin region (Faulds et al. 2013). Though there are no active natural thermal features in the vicinity of San Emidio, evidence for geothermal capacity was identified associated with significant surface alterations and hydrothermal deposits. A prominent example is the Wind River gold and silver mine – historically operated to the NNW of the current system – which is located in another of the right-stepping fault bends north of the current reservoir. In the shallow subsurface, a zone of significant range-parallel silicified and altered sediment (Qas) has also been recognized as evidence of geothermal fluid outflow toward the north (Rhodes 2011).

Early exploration of the field occurred in the 1970s, and temperature gradient measurements via shallow wells indicated a fault-parallel high-temperature (>100°C) system within 30m of the land surface (Figure 1, inset). Deeper drilling has occurred since the mid-1970s, with mixed success in reaching both temperatures and permeabilities necessary for efficient extraction and electricity generation. During deepening to 555m of one production well (75-16) in 1994, deep permeability and temperature conditions viable for geothermal energy production were encountered (Matlick 1995). Since this initial discovery, several other wells drilled to the south of 75-16 have encountered significant permeability and high temperatures, expanding access to the geothermal resource. Since 2018, the site has been owned and operated by ORMAT Technologies, Inc. following its acquisition of the prior owner, U.S. Geothermal.

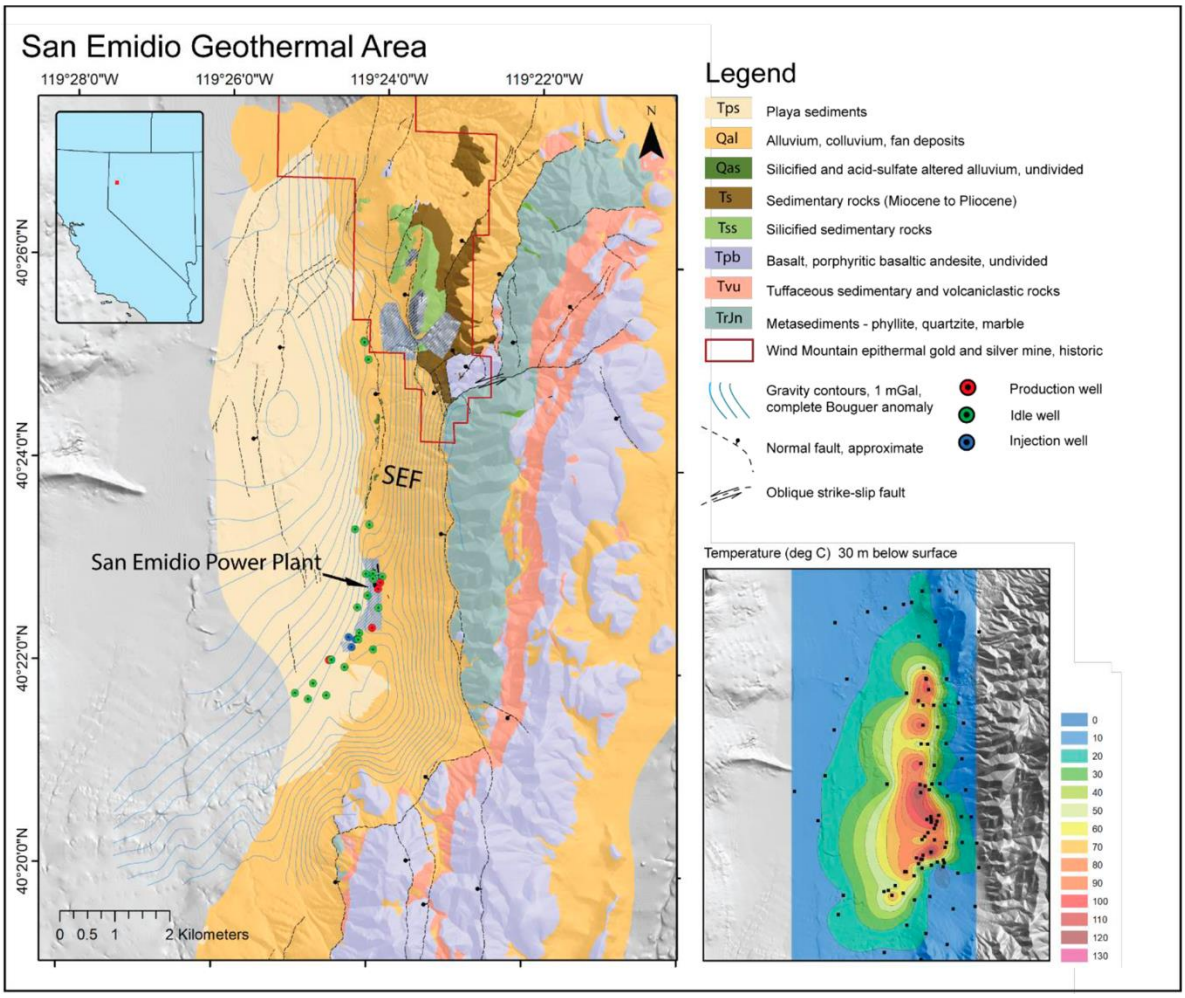

Figure 1: Geologic site setting and surficial exposures of the San Emidio Geothermal Field from Folsom et al. (2020) (as modified from Rhodes et al. (2011)). Inset map shows contouring of shallow temperature anomaly mapped via temperature gradient wells.

The WHOLESCALE project is an industry-university collaborative effort that seeks to understand the evolution of stress within geothermal reservoirs, a key prerequisite to understanding seismicity in these systems (Feigl et al. 2022). In studying the San Emidio system, all data and research products are referenced to the WHOLESCALE coordinate system. Laterally, the origin of the coordinate system is UTM Zone 11T [Easting, Northing] = [286924.276803259m, 4457966.68897815m]. Vertically, WHOLESCALE results are referenced as orthometric height above mean sea level (AMSL, WGS 84 geoid) in meters.

ORMAT Technologies, Inc. (henceforth, ORMAT), as the industry partner on the WHOLESCALE project, has shared information with the project team uncluding well assemblies, current site operations and pumping rates, and a site conceptual model that represents the 3-D geometry of the San Emidio system (Figure 2). Major infrastructure operated at the site from 2016 onward includes: 1) four production wells (75B-16, 76-16, 61-21, and – since 2018 – 25A-21) targeting depths from approximately 100m to 930m below land surface; and 2) three shallow wells (42-21, 43-21, and 53-21) where water is re-injected under ambient pressure. Other inactive wells that access the reservoir are shown in black in Figure 2, and represent locations where reservoir pressure changes can be monitored. Pressure change data from pumping tests in 2016 and 2017 were recorded by ORMAT independently, and provided as part of the WHOLESCALE project. Most recently, observed pressure changes were recorded at 13 inactive wells during the 2022 site shutdown as part of the WHOLESCALE project.

In this study, we analyze the historical pumping test data from San Emidio, as provided by ORMAT, to estimate spatially variable subsurface permeability. The geologic structural model contains the key stratigraphic units and fault structures identified via geologic and geophysical analysis of the region. We pursue multiple conceptual models for the dominant drivers of permeability variability through alternative parameterizations of subsurface structures represented in this model. Using the pumping test data sources, we perform forward modeling using the COMSOL Multiphysics finite element modeling platform, and estimate – through inverse modeling – the permeability of key geologic structures. The results of forward and inverse modeling are used to simulate pressure changes expected during plant shutdowns in 2016, 2021, and 2022, which contributes to changes in effective stress on faults. In future work, we will compare the results of the simulated pressure changes against the hypocenters and timing of microseismic events observed during each of these shutdowns.

Together, these data sources provide evidence for the current state of stress in the San Emidio geothermal reservoir as well as its evolution over time.

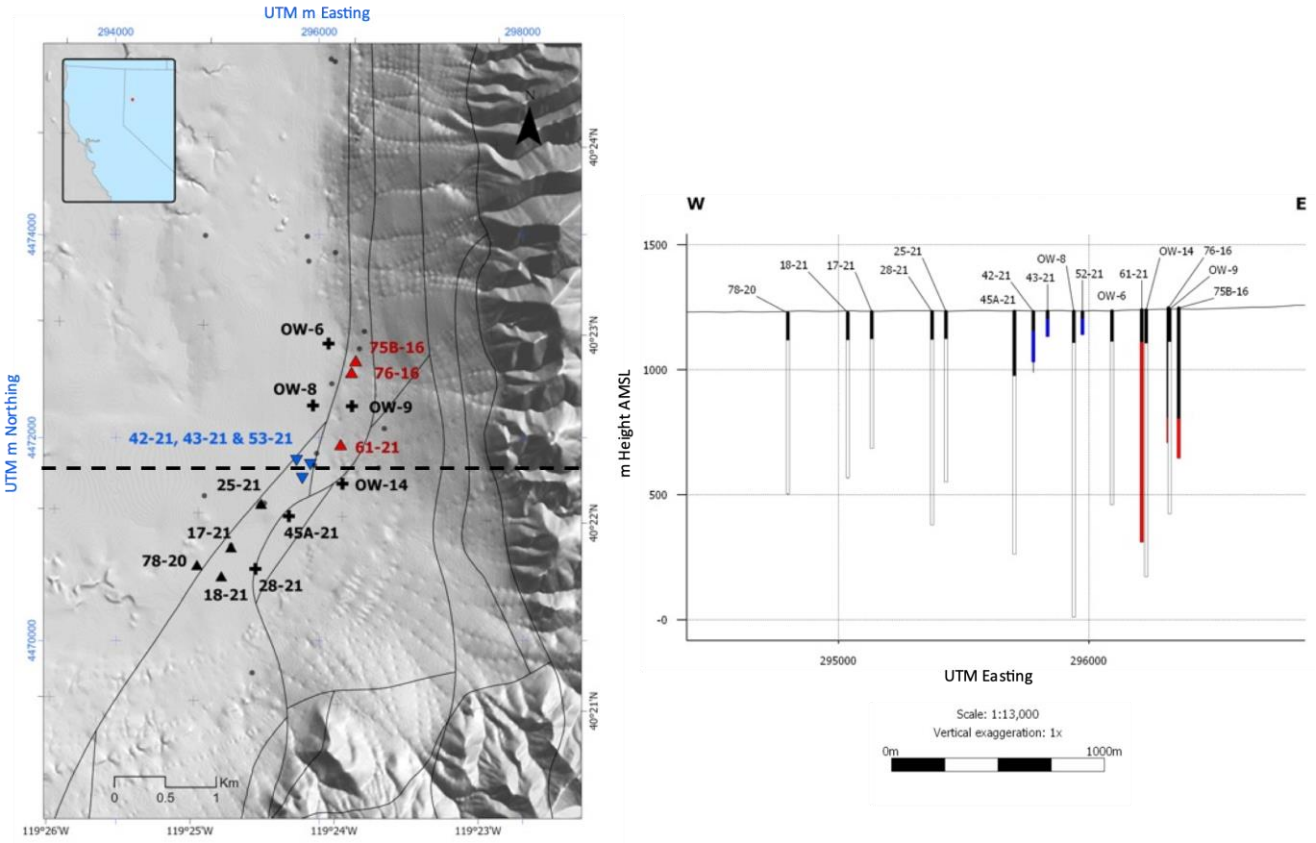

Figure 2: Site infrastructure active during 2016. Left: Map-view locations of all active wells relative to estimated fault traces. Right: Well locations, projected to a plane of UTM Zone 11T 4,471,700m N. Elevation is orthometric height above mean sea level (WGS 84 geoid)

2. METHODS

The geologic conceptual model of the subsurface provided by ORMAT was developed in Leapfrog Geothermal, and includes geometric elements that define key volumes (lithology), surfaces (faults and lithologic boundaries) and curves (wellbore profiles). Five key stratigraphic units are defined (Figure 3, left), as documented by Folsom et al. (2020) – from deepest to shallowest, they are: 1) Triassic and Jurassic Nightingale metasedimentary rocks (TrJn) consisting of phyllite, quartz, and marble; 2) Tertiary andesites and tuffaceous units (Tvu); 3) Tertiary basalt (Tpb); 4) Quaternary alluvial fill (Qal); and 5) Altered and silicified Quaternary alluvial sediments (Qas) that represent the shallow north-trending geothermal outflow zone (Rhodes 2011; Folsom et al. 2020). Key faults that are thought to be important contributors to fluid flow in the region (Figure 3, right) are the San Emidio Fault (SEF) and Basin Bounding Fault (BBF), which were parameterized as permeable through all units except the Nightingale basement material (TrJn). This geologic conceptual model was imported into the COMSOL Multiphysics models and translated to the WHOLESCALE coordinate system described above.

Information provided by ORMAT for each well at the site included the UTM coordinates at land surface, the total depth of drilling, and the range of depths over which the well is open to the surrounding formation (either via a perforated interval or open hole). For pumping tests performed in 2016 and 2017, flow rates at all pumping wells and pressure responses at a subset of site wells representing observation wells were provided. For site shutdowns, flow rate data from all operational (i.e., producing and injecting) wells was provided. A summary of the pressure data utilized is found in Table 1, and an example of the 2017 testing data is shown in Figure 4. Before importing into the COMSOL model, all pumping data was converted to mass estimates by assuming a fluid density for water at 100°C. Pressure change observations were baselined to assume zero pressure change before pumping changes began, and then resampled to hourly time steps.

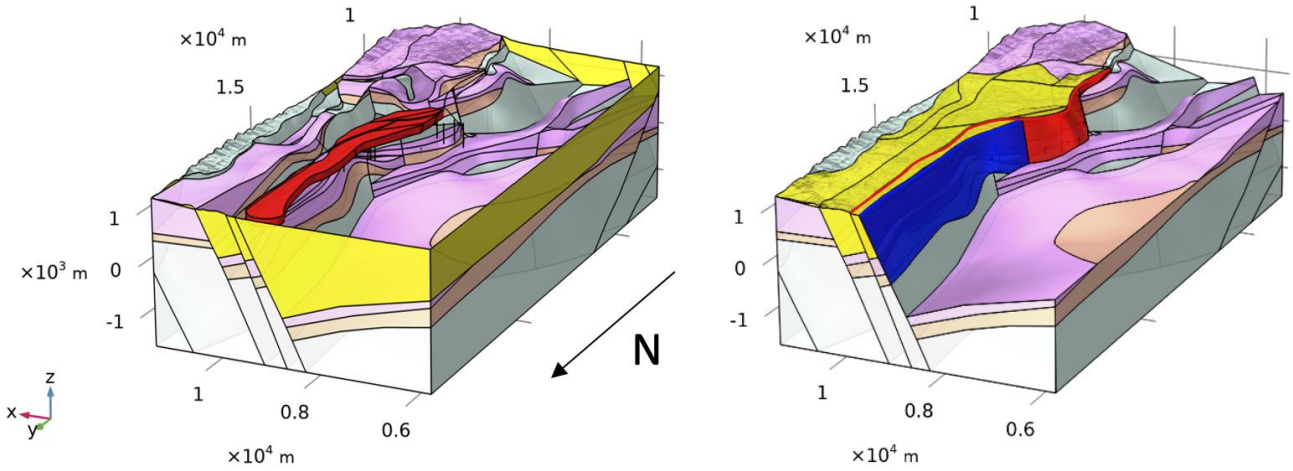

Figure 3: Two views of geologic conceptual model (camera is from the northwest) provided by ORMAT. Left: Stratigraphic geologic units are from top to bottom: Qal (yellow, with land surface removed), Qas (red), Tbp (pink), Tvu (orange) and TrJn (teal). Right: Fault planes considered as permeable segment SEF (red) and BBF (blue).

Table 1: Testing data utilized within COMSOL finite element numerical model.

	2016 Testing	2017 Testing	2016 Site Shutdown
Time Period Imported	2016-10-05 – 2016-10-13	2017-09-19 – 2017-09-27	2016-12-07 – 2016-12-15
Pumping Flow rates	17-21, 25-21	17-21, 18-21, 78-20	61-21, 75B-16, 76-16 (Production) 42-21, 43-21, 53-21 (Injection)
Pressure Observations	OW-6, OW-8, OW-9	OW-6, OW-8, OW-9, 25-21, 28-21, 45A-21	None

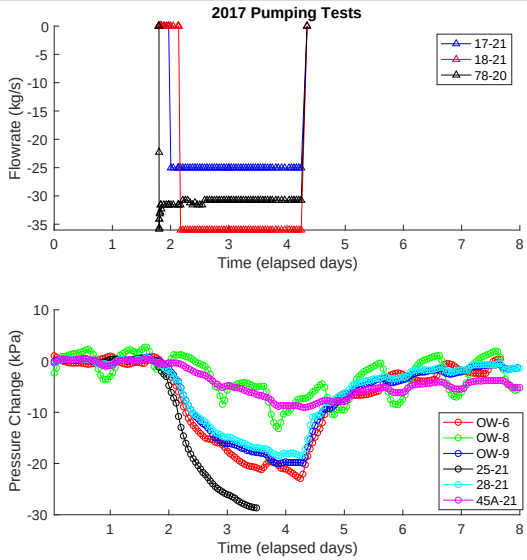

Figure 4: 2017 flow rate (positive flowrate is injection, negative is production) and pressure data provided by ORMAT, after units conversion and baselining. Elapsed days are days after 2017-09-19

Once all geometry, hydraulic forcing, and observational data were imported to COMSOL, the model domain was discretized using tetrahedral finite elements using COMSOL's automatic meshing routines. Several meshes were created, and the mesh used depended on the time period being simulated. For the experimental pumping tests, the mesh was refined near wells 17-21, 18-21, and 78-20 as these represented the location of pumping and thus the steepest expected head gradients. For later modeling of site shutdowns (described in the

"Results" section below), the mesh was refined in the vicinity of all operational wells. The mesh is conformal with the geologic boundaries shown in Figure 3, and is also refined in the vicinity of all operational wells to have a maximum dimension of 50m.

After validating the numerical model through mass balances and other solution checks, the COMSOL model was used to perform inverse modeling for the internal permeability structure. Other model parameters – including stratigraphic unit porosity, effective matrix compressibility, fluid viscosity, fluid density, and fluid compressibility – were assumed constant, based on either prior site data or (where unavailable) literature estimates. Permeability was parameterized according to a series of alternative conceptual models, following the approach of multiple working hypotheses (Chamberlin 1890). In conceptual model 1 (CM1), which is used as a baseline, the reservoir assumes a homogeneous, anisotropic permeability value throughout the region. For conceptual models 2 through 4 (CM2 – CM4), stratigraphic and structural permeability variations are successively included. In CM2, we estimated permeability values for each stratigraphic unit (TrJn, Tvu, Tpb, Qal, and Qas), along with a vertical anisotropy coefficient for all units (representing the ratio of horizontal to vertical permeability). In conceptual model 3 (CM3), an additional permeability value was added to represent the San Emidio Fault (SEF) as a fault plane with its own permeability and assumed fault zone of 1 m width. In conceptual model 4, we include both the mapped San Emidio Fault (SEF) and basin bounding fault (BBF) as units with their own defined permeability values, each also with $1m$ widths. All individual forward run simulations required less than 10 minutes on a 2.5 GHz, 28-core Intel Xeon W computer with 96GB of RAM. At present, the model simulates fluid flow only, though COMSOL is capable of coupled thermal-hydraulic modeling, which is planned for the future.

All observations of pressure change during the 2016 and 2017 pumping tests were fit via inversion using nonlinear least squares. We minimized the least squares objective function using an iteratively linearized Gauss-Newton method, which approximates the objective function as quadratic in the vicinity of current parameter estimates (e.g., Aster et al. 2005). To ensure non-negativity of input permeability, all inverse modeling was performed on log-transformed parameter values, which were converted back into native units following convergence. During each inversion iteration, the elements of the model Jacobian matrix – representing the sensitivity of all simulated observations to all model parameters – were estimated via a finite difference method that successively altered each parameter by 30%. Iteration in the inversion included a line-search between current parameter estimates and the update step calculated via Gauss-Newton. Convergence was declared when the maximum relative parameter change was less than 0.1% or when the relative objective function change was less than 0.1% at the end of a linearization iteration. Full inversion runtimes for each conceptual model were several days each.

Different pumping and injection locations were operating during the 2016 site shutdown, and at larger flow rates than those recorded during the 2016 and 2017 pumping tests. No pressure observations were recorded for the 2016 shutdown, however, increased microseismicity at the site during the 2016 shutdown suggest that stress changes caused by pumping cessation altered the effective stress, promoting slip on fault planes. To assess the likely pressure changes within the reservoir following pumping cessation, we use the optimized parameters in the numerical model to simulate pressure changes expected in the San Emidio reservoir following the altered flow rates caused by the 2016 site shutdown, which lasted approximately 1 day.

3. RESULTS

Results for all inversions are summarized in Table 2, including the root mean squared error (RMSE) misfit between hourly-resampled observations of pressure changes and model-simulated pressure changes. Analyses of data from periods when site operations do not change had an average standard deviation of 1.4 kPa; this value is thus assumed as a reasonable proxy for inherent "measurement error" associated with unmodeled processes including sensor noise, systematic drift, and secular signals including atmospheric temperature fluctuations that affect instrument response.

While overall RMSE for each model is of the same order of magnitude as sensor error, plots of drawdown curves for individual observation wells indicate potential structural errors in all conceptual models. For both the 2016 and 2017 pumping tests, pumping took place toward the southern end of the wellfield. Field data indicates that pressure response at northern well OW-6 was similar in magnitude and timing to pressure response at well 28-21 in the south (Figure 5). Another northern well, OW-8, experienced very small pressure variation despite its proximity to OW-6. All inverse modeling results, however, simulated small pressure changes at northern well OW-6. These observations taken together suggest that flow conduits connecting the southern field to OW-6 at its open interval may be present that are currently not represented in the geologic conceptual structure.

All heterogeneous conceptual models show improvement in reducing data misfit relative to the homogeneous base case (CM1). Though it does not include any fault-based permeability, CM2 is consistent with other observations from prior studies at San Emidio, including: 1. Qas (silicified alluvium) has been previously identified as unit that likely has substantial permeability relative to other basin-fill materials; and 2. the permeability anisotropy ratio of approximately 3 for all geologic units is within a reasonable range for natural sediment and rock formations. In contrast, CM3 includes the San Emidio Fault (SEF) and estimates high permeability for this feature, but: 1. Qas is optimized as having lower permeability than surrounding materials, which is not consistent with other observations; and 2. The anisotropy ratio, which implies a >1000-fold decrease in vertical hydraulic conductivity, is significantly more extreme than even those observed in shales over a range of pressure conditions (Pan et al. 2015; Bhandari et al. 2015). Finally, CM4 includes both the San Emidio Fault (SEF) and Basin Bounding Fault (BBF) as separate permeable units. This conceptual model is able to obtain a similar level of misfit to CM2 and CM3, and we deem this model to be more plausible than CM3 due to: 1. a high permeability estimated for Qas, as in CM2; and 2. A more reasonable estimated anisotropy ratio.

Table 2: Results of inverse modeling from all 4 conceptual models.

	*CM1**	*CM2*	*CM3*	*CM4*
RMSE Misfit $[kPa]$	5.8	5.2	5.3	5.3
Qal $k_x[m^2]$	2.9×10^{-12}	1.5×10^{-13}	1.9×10^{-13}	1.5×10^{-13}
Qas $k_x\ [m^2]$	2.9×10^{-12}	6.2×10^{-11}	5.0×10^{-15}	4.3×10^{-11}
Tpb $k_x\ [m^2]$	2.9×10^{-12}	1.3×10^{-13}	2.0×10^{-13}	1.7×10^{-12}
Tvu $k_x\ [m^2]$	2.9×10^{-12}	5.2×10^{-11}	1.4×10^{-10}	2.4×10^{-11}
TrJn $k_x\ [m^2]$	2.9×10^{-12}	4.4×10^{-14}	4.4×10^{-14}	3.1×10^{-14}
Anisotropy $\frac{k_x}{k_z}$	2.0	3.5	1,300	140
SEF $k\ [m^2]$	–	–	1.7×10^{-10}	4.4×10^{-11}
BBF $k\ [m^2]$	–	–	–	3.7×10^{-9}

**Permeability for all stratigraphic units (Qal, Qas, Tpb, Tvu, TrJn) was estimated as a single parameter in CM1*

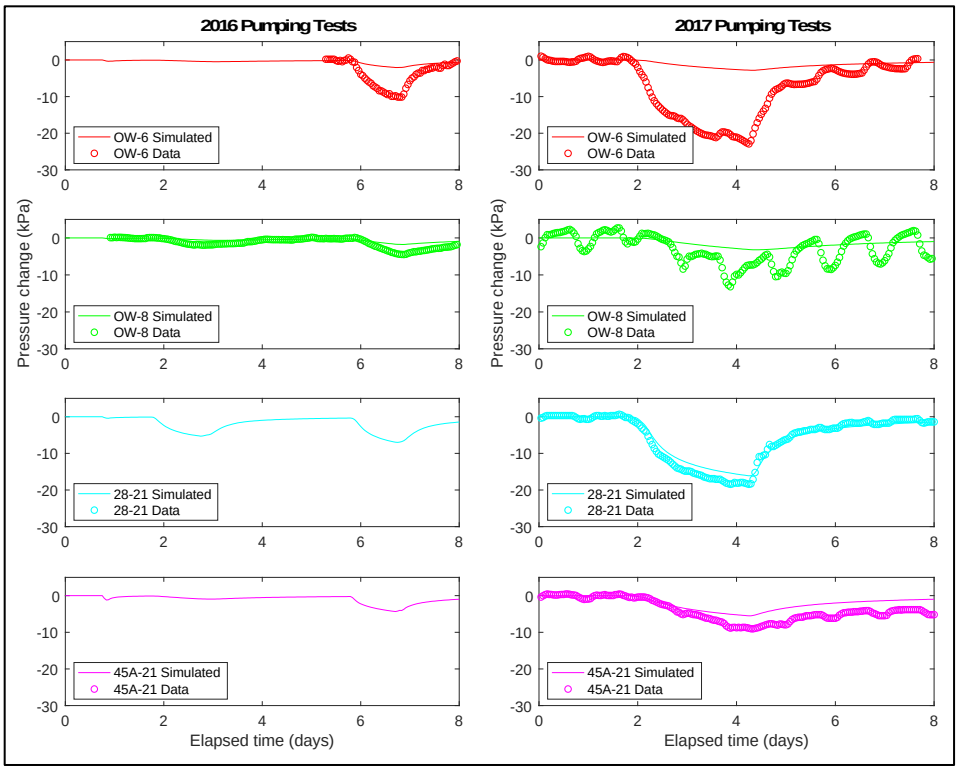

Figure 5: Simulated pressure changes from CM2 (lines) and resampled pressure observations (symbols) for subset of pressure data from 2016 and 2017 pumping experiments. Impacts from atmospheric temperature fluctuations on observations is prominent in 2017 OW-8 observations. Elapsed days represent days after start of time period described in Table 1.

Following inverse modeling, we can use these forward models with the associated permeability estimates to simulate the impact of pumping shutdowns on site pressure changes. In this work, we present a simulation of pressure changes following the 2016 site shutdown (Figure 6 – left), which took place on days 2016-12-08 and 2016-12-09 UTC. Prior to site shutdown, total flow rates at San Emidio were approximately 0.3 m^3/s, with all extracted water (from wells 61-21, 75B-16, and 76-16) being returned via injection wells (42-21, 43-21, and 53-21). Considered relative to long-term site operations, this shutdown produces an increase in pore pressure near production wells and a decrease near injection wells. Pressure changes relative to normal site operations – as simulated by our COMSOL model, CM2 – are shown immediately before normal operations resumed (Figure 6 – right). Pressure changes up to approximately 40kPa are transmitted several hundred meters from the pumping well intervals, and pressure changes of 10kPa extend over roughly 1km laterally immediately before pumping resumes.

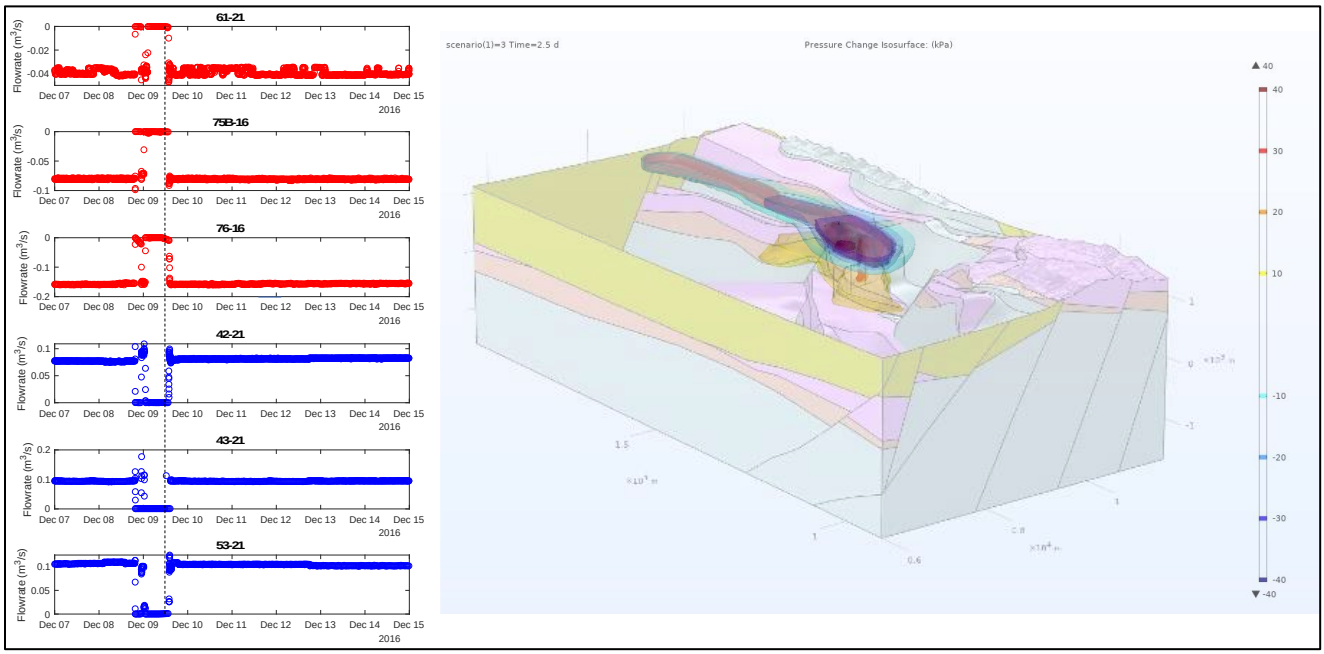

Figure 6: Flow rate changes during 2016 shutdown (positive flow rate = injection) Right: Pressure change isosurfaces (red = positive) overlain on structural model, simulated using CM2. Simulating time snapshot corresponds to dashed line on flowrate plot.

Other results presented during this meeting estimate hypocentral locations of microseismic events recorded in 2016 during the site shutdown; the majority of these microseismic events occurred between 6 and 12 hours after the site shutdown began. In ongoing work, we will compare the location and timing of microseismic events against the simulated pressure changes within the San Emidio reservoir.

4. CONCLUSIONS AND FUTURE WORK

Many physical parameters required as inputs to geothermal reservoir simulators are well constrained, when considered relative to reservoir permeability. Bulk thermal conductivity, volumetric heat capacity, bulk compressibility, porosity, and temperature-dependent water density and viscosity each contribute to determining fluid and heat transport in the subsurface, though each seldom experiences more than an order of magnitude variability within natural fluids and geologic materials comprising geothermal reservoirs. In contrast, permeability commonly varies by 2 orders of magnitude or more even within a single geologic material (e.g., Freeze and Cherry 1979), and the connectivity of high-permeability pathways in geothermal reservoirs exerts a dominant control on the shape and efficiency of the subsurface "heat exchanger". Efforts to better understand heat, pressure, and effective stress evolution in geothermal reservoirs are thus crucially dependent on an accurate model of subsurface permeability structures.

In this paper we employed existing site geologic conceptual models and tested multiple parameterizations of spatially variable permeability within this framework. We employed four conceptual models, ranging from a homogeneous but anisotropic half-space to a heterogeneous model that included multiple stratigraphic layers and fault units, each with their own permeability. Each heterogeneous model improved somewhat upon the homogeneous model (CM1), in terms of fit to existing pumping test data, though no model was able to fit all pressure data to within expected measurement error. Future improvements to fitting pressure data may be possible with an updated structural model of subsurface formations. Alternatively, highly parameterized permeability models with a regularization term to reduce impacts of illposedness may be employed as a more flexible strategy for matching observed pressure observations, as is employed in hydraulic tomography (Cardiff et al. 2012, 2013).

Once permeability is estimated or "tuned" via inverse modeling of an appropriate series of pumping tests, the reliability of pressure change simulations is expected to increase. Forward modeling of site operation with these tuned models can then be used to more reliably simulate the effect of wellfield operations – such as site shutdowns for maintenance – on reservoir stresses, and the associated slip tendencies on faults. Multiple datasets that reflect hydro-mechanical processes – including reservoir deformation, seismicity, fluid temperature and fluid pressure data – provide further opportunity to update site conceptual models and improve this forward modeling, especially if collected synoptically. Future work will utilize the 2022 data collected by the WHOLESCALE project which includes an expanded set of pressure observations, seismic measurements from seismographs, and deformation observations from GPS and InSAR, all collected throughout the 2022 shutdown at San Emidio.

ACKNOWLEDGMENTS

The WHOLESCALE team thanks the following individuals at Ormat Technologies: Curtis Peach, Cliff Reed, Joe Pavone, Manolo Di Donato, Leeta Miller, Alan Pinuelas-Molina, David Schwab, Lupé Gonsalez Ortiz, Gabrielle Ramirez, Courtney Brailo, Zack Young, John Murphy, John Akerly, and Robin Zuza.

The work presented herein has been funded in part by the Office of Energy Efficiency and Renewable Energy (EERE), U.S. Department of Energy, under Award Numbers DE-EE0007698 and DE-EE0009032.

REFERENCES

Aster, R. C., B. Borchers, and C. H. Thurber. 2005. *Parameter Estimation and Inverse Problems*. Vol. 90. International Geophysics Series.

Bhandari, A. R., P. B. Flemings, P. J. Polito, M. B. Cronin, and S. L. Bryant. 2015. Anisotropy and Stress Dependence of Permeability in the Barnett Shale. *Transport in Porous Media* 108, no. 2: 393–411, https://doi.org/10.1007/s11242-015-0482-0.

Cardiff, M., W. Barrash, and P. K. Kitanidis. 2012. A field proof-of-concept of aquifer imaging using 3D transient hydraulic tomography with temporarily-emplaced equipment. *Water Resources Research* 48: W05531, https://dx.doi.org/10.1029/2011WR011704.

Cardiff, M., W. Barrash, and P. K. Kitanidis. 2013. Hydraulic conductivity imaging from 3-D transient hydraulic tomography at several pumping/observation densities. *Water Resources Research* 49, no. 11: 7311–26, https://dx.doi.org/10.1002/wrcr.20519.

Cardiff, M., D. Lim, J. R. Patterson, J. Akerley, P. Spielman, J. Lopeman, P. Walsh, et al. 2017. Geothermal production and reduced seismicity: Correlation and proposed mechanism. *Earth and Planetary Science Letters* 482: 470–77, https://doi.org/10.1016/j.epsl.2017.11.037.

Chamberlin, T. C. 1890. The method of multiple working hypotheses. *Science*, no. 366: 92–96.

Faulds, J. E., C. D. Henry, and N. H. Hinz. 2005. Kinematics of the northern Walker Lane: An incipient transform fault along the Pacific–North American plate boundary. *Geology* 33, no. 6: 505, https://doi.org/10.1130/G21274.1.

Faulds, J. E., N. H. Hinz, G. M. Dering, and D. L. Siler. 2013. The Hybrid Model—The Most Accommodating Structural Setting for Geothermal Power Generation in the Great Basin, Western USA. *Geothermal Resources Council Transactions* 37: 3–10.

Feigl, K. L., S. Tung, H. Guo, E. Cunningham, J. Hampton, S. J. Kleich, B. Jahnke, et al. 2022. Overview and Preliminary Results from the WHOLESCALE project at San Emidio, Nevada, U.S. *PROCEEDINGS, 47th Workshop on Geothermal Reservoir Engineering*. Stanford, CA, USA, https://doi.org/10.7932/NCEDC.

Folsom, M., R. Libbey, D. Feucht, I. Warren, and S. Garanzini. 2020. Geophysical Observations and Integrated Conceptual Models of the San Emidio Geothermal Field, Nevada. In *PROCEEDINGS, 45th Workshop on Geothermal Reservoir Engineering*, SGP-TR-216.

Freeze, R. A., and J. A. Cherry. 1979. *Groundwater*. Englewood Cliffs, N.J: Prentice-Hall.

Matlick, J. S. 1995. San Emidio Geothermal System, Empire, Nevada: GRC Field Trip ~ October 1995.

Pan, Z., Y. Ma, L. D. Connell, D. I. Down, and M. Camilleri. 2015. Measuring anisotropic permeability using a cubic shale sample in a triaxial cell. *Journal of Natural Gas Science and Engineering* 26, September: 336–44, https://doi.org/10.1016/j.jngse.2015.05.036.

Rhodes, G. T. 2011. Structural Controls of the San Emidio Geothermal System, Northwestern Nevada. University of Nevada, Reno, http://hdl.handle.net/11714/4011.

Rhodes, G. T., J. E. Faulds, and A. R. Ramelli. 2011. Preliminary Geologic Map of the Northern Lake Range, San Emidio Geothermal Area, Washoe County, Nevada. 11–11. Open-File Report.